Contribution from the Department of Chemistry, University of Chicago, 5735 South Ellis Avenue, Chicago, Illinois 60637, and Inorganic Chemistry Laboratory, University of Oxford, South Parks Road, Oxford OX1 3QR, United Kingdom

Splitting of Cluster Orbitals

David J. Wales*,† and D. Michael P. Mingos‡

Received October 27, 1988

The splitting of cluster orbitals is discussed within the framework of Stone's tensor surface harmonic (TSH) theory. We proceed by analogy with the splitting of spherical harmonics subject to the same potential. We show how the energy level spectrum of a cluster compound correlates with its shape and discuss both *closo*-boranes and gold clusters in this context, making comparisons with molecular orbital calculations. The approach provides a particularly elegant description of the variation in electron count of a series of related gold clusters. It also enables us to rule out certain rearrangement pathways for toroidal gold clusters; for example, we find that oblate toroidal gold clusters cannot rearrange through a prolate transition state for reasons of orbital symmetry.

Introduction

In recent years Stone's tensor surface harmonic (TSH) theory[1-3] has proved to be a highly versatile tool in the discussion of the bonding in cluster compounds. In particular the method has been used to provide a firmer theoretical foundation for empirical rules of cluster electron counting such as the *Debor principle*[4] and the *polyhedral skeletal electron pair theory*.[5] Comparisons have also been made[6] with King's graph-theoretical approach.[7]

In brief, TSH theory is based upon an approximate descent in symmetry from the full rotation group. Basis functions are classified as σ, π, and δ according to the number of nodal planes they possess that contain the radius vector from the center of the cluster to the atom. Cluster orbitals are formed from σ-type basis functions (which contain no nodal planes containing the radius vector) by using the values of spherical harmonics evaluated at the cluster vertices as expansion coefficients. A useful comparison may be made with the Hückel wave functions for cyclic and linear polyenes: the appropriate linear combinations can be obtained from the wave functions for a free electron on a ring or in a box, respectively. For an approximately spherical cluster, we use the eigenfunctions for a free electron on a sphere in a similar manner to construct and classify cluster wave functions. For example, a σ cluster orbital, $\psi^{\sigma}_{L,M}$ is given by

$$\psi^{\sigma}_{L,M} = \sum_i Y_{L,M}(\theta_i,\phi_i)\ \sigma(i) \qquad (1)$$

where θ_i and ϕ_i are the angular spherical polar coordinates of vertex i.

To deal with π- and δ-type basis functions (with one and two nodal planes containing the radius vector, respectively), we proceed in a similar manner but use the values of tensor surface harmonics as expansion coefficients. For π cluster orbitals (with one nodal plane containing the radius vector) the gradient vector is evaluated at each vertex and gives the required coefficients when resolved in the directions of, e.g., two tangential p orbitals. Further details may be obtained elsewhere.[1-3]

More recent developments include the development of a structural TSH model[6] and the use of TSH theory in the discussion of cluster rearrangements.[8]

The most important characteristic of the TSH theory cluster orbitals for the present work is their transformation under rotations. For $\psi^{\lambda}_{L,M}$ ($\lambda = \sigma, \pi, \delta$) the L and M subscripts reflect the parentage of the orbital under spherical symmetry, where they are good quantum numbers. In a finite point group, we find that functions with different L or M do not mix with each other very strongly, and hence L and M are useful symmetry labels. Furthermore, the cluster orbitals transform under rotations of the point group in the same way as the parent spherical harmonic upon which the expansion coefficients are based. Under reflections, inversions, and other "improper" symmetry operations, they may transform in the same way or with a change of sign. However, the cluster orbitals do not transform in the same way as the spherical harmonics under arbitrary rotations. This is because rotations that do not belong to the molecular point group move the centers for the atomic orbitals in the linear expansion.

A number of powerful theoretical results may be applied to Hamiltonian (or indeed overlap) matrix elements of functions which *do* transform like the spherical harmonics under arbitrary rotations by using the Wigner-Eckart theorem.[9] Strictly speaking, the spherical harmonics are *spherical tensors*, and the matrix element theorems that may be applied are the same as those used in finding general selection rules in spectroscopy. These results may be used to prove a barycenter (center of gravity) rule for the splitting of such functions in finite point groups. We will argue that the splitting of cluster orbital manifolds, $\psi^{\lambda}_{L,M}$, should be qualitatively similar and will show how this conclusion leads us very simply to a number of interesting observations, including the correlation of the energy level spectrum of a cluster with its shape and the rationalization of the electron counts of various gold clusters.

Expansion of the Electron-Nucleus Potential Energy

The Coulomb interactions between an electron, i, and a set of N nuclei may be expanded in a series of spherical harmonics:

$$V = -\sum_{\alpha=1}^{N} \frac{Z_\alpha}{r_{i\alpha}} = -\sum_{\alpha=1}^{N} \sum_{L=0}^{\infty} \sum_{M=-L}^{L} Z_\alpha \frac{4\pi(-1)^M}{2L+1} \frac{r_{i<}^L}{r_{i>}^{L+1}} Y_{L,M}(\theta_i,\phi_i)\ Y_{L,-M}(\theta_\alpha,\phi_\alpha) \qquad (2)$$

where Z_α is the atomic number of nucleus α, $r_{i\alpha}$ is the distance between electron i and nucleus α and $r_{i<}$ and $r_{i>}$ are the smaller and larger of the distances of the electron and the nucleus in question from the origin, respectively. Atomic units are employed for convenience (one atomic unit of energy (1 hartree) equals 27.2 eV). Such an expansion has been used extensively in the crystal

† University of Chicago.
‡ University of Oxford.

(1) Stone, A. J. *Mol. Phys.* **1980**, *41*, 1339.
(2) Stone, A. J. *Inorg. Chem.* **1981**, *20*, 563. Stone, A. J.; Alderton, M. J. *Inorg. Chem.* **1982**, *21*, 2297. Stone, A. J. *Polyhedron* **1984**, *3*, 1299. Mingos, D. M. P.; Wales, D. J. *Introduction to Cluster Chemistry*; Prentice-Hall: Englewood Cliffs, NJ; in press.
(3) Wales, D. J.; Stone, A. J. *Inorg. Chem.*, in press.
(4) Williams, R. E. *Prog. Boron Chem.* **1970**, *2*, 51. Williams, R. E. *Inorg. Chem.* **1971**, *10*, 210. Williams, R. E. *Adv. Inorg. Chem. Radiochem.* **1976**, *18*, 67. Wade, K. *J. Chem. Soc., Chem. Commun.* **1971**, 792. Rudolph, R. W.; Pretzer, W. R. *Inorg. Chem.* **1972**, *11*, 1974. Rudolph, R. W. *Acc. Chem. Res.* **1976**, *9*, 446.
(5) Mason, R.; Thomas, K. M.; Mingos, D. M. P. *J. Am. Chem. Soc.* **1973**, *95*, 3802. Mingos, D. M. P. *Nature (London), Phys. Sci.* **1972**, *236*, 99.
(6) Stone, A. J.; Wales, D. J. *Mol. Phys.* **1987**, *61*, 747. Wales, D. J. *Mol. Phys.*, in press.
(7) King, R. B. *Inorg. Chem.* **1988**, *27*, 1941.
(8) Wales, D. J.; Stone, A. J. *Inorg. Chem.* **1987**, *26*, 3845.
(9) See, e.g.: Weissbluth, M. *Atoms and Molecules*; Academic Press: New York, 1978.

0020-1669/89/1328-2748$01.50/0 © 1989 American Chemical Society

field theory of transition-metal complexes,[10] and although the expansion appears to be rather complicated, the number of significant terms is often quite small for highly symmetrical clusters. It has also been used before by Hoffmann and Gouterman in their perturbation theory approach to the energy levels of polyhedral molecules.[11]

The Coulombic electron–nucleus potential energy, V, may therefore be written as a sum of two terms:

$$V = V_0 + V_1 \tag{3}$$

where $V_0 = -4\pi\sum_\alpha Z_\alpha/r_>$ and V_1 denotes the remainder of V. V_0 is clearly the part of V that is unchanged by all the operations of the full rotation group, and the same separation is used in ligand-field theory.[12] For example, it is well-known that the significant part of V_4 for an octahedral transition-metal complex is usually written

$$V_{oct} \propto Y_{4,0} + \sqrt{\frac{5}{14}}(Y_{4,4} + Y_{4,-4}) \tag{4}$$

Taking V_0 together with the kinetic energy terms gives us a zero-order Hamiltonian in which all the operators transform according to the irreducible representation S_g of the full-rotation group. Hence, to establish our barycenter rule for the first-order splittings of a set of $2L + 1$ spherical harmonics, $Y_{L,M}$ ($M = -L$ to $+L$), we must show that the functions are not split by V_0 and that the first-order energy corrections under the perturbation V_1 sum to zero. In fact, these results follow immediately from the transformation properties under rotations, but since they may not be familiar to cluster chemists, we will explain them below.

First, consider the matrix elements of V_0 within the $Y_{L,M}$ manifold. The Wigner–Eckart theorem[9] states that

$$\langle J'M'|T^K_Q|JM\rangle = \langle JKMQ|J'M'\rangle\langle J'||T^K||J\rangle \tag{5}$$

where $\langle JKMQ|J'M'\rangle$ is a Clebsch–Gordan coefficient and $\langle J'||T^K||J\rangle$ is a reduced matrix element that is independent of M, M', and Q. T^K_Q is a spherical tensor of rank K and in the present work will always be a spherical harmonic, $Y_{K,Q}$. Since V_0 is proportional to $Y_{0,0}$, K and Q are both zero for this term, and the matrix elements of V_0 therefore depend only upon the Clebsch–Gordan coefficients $\langle L0M0|LM'\rangle$. However, for a general Clebsch–Gordan coefficient to be nonzero, two conditions must be satisfied: (a) It must be possible to make a triangle with sides of length J, J', and K; that is, the sum of any pair of principal quantum numbers must be greater than or equal to the third.

(b) We must have $M' = M + Q$. For V_0, the first condition is satisfied, and the second requires $M = M'$, so that there are no off-diagonal matrix elements. Furthermore, the diagonal matrix elements are all equal because[9]

$$\langle L0M0|L-M\rangle = 1 \tag{6}$$

The reader could rightly complain that in this case we have "used a sledgehammer to crack a nut", since it is clear that a Hamiltonian containing only terms that transform as S_g in the full rotation group cannot lift the $(2L + 1)$-fold degeneracy of the spherical harmonics, $Y_{L,M}$, which are the irreducible representations of this group. The example above was really given for illustration of how one may use the Wigner–Eckart theorem in a simple case.

It is actually not much harder to prove the second part of the barycenter rule. We have shown that the zero-order Hamiltonian matrix is diagonal within a given $Y_{L,M}$ manifold and that the diagonal elements are all the same. Let us choose our origin of energy at the zero-order energy of the $Y_{L,M}$ set and apply degenerate perturbation theory for the term V_1. This simply means that we diagonalize the secular matrix of V_1. For a barycenter rule to hold, we must show that the sum of the eigenvalues of this secular determinant is zero. Since the sum of the eigenvalues, ϵ_i, is the trace of the secular matrix with diagonal elements $\langle LM|V_1|LM'\rangle$, we have

$$\sum_i \epsilon_i = \sum_{M=-L}^{M=L} \langle LM|V_1|LM\rangle \tag{7}$$

The right-hand side vanishes because the sum $\sum_M Y_{L,M}Y^*_{L,M}$ transforms as S_g in the full-rotation group (like a filled atomic subshell), whereas V_1, by definition, does not. Hence, we have demonstrated that a barycenter rule applies to the first-order splitting in an arbitrary potential of the $2L + 1$ spherical harmonics $Y_{L,M}$, that is before interaction between functions with different L is admitted. The great utility of TSH theory is, of course, that these latter interactions are generally small for cluster orbitals.

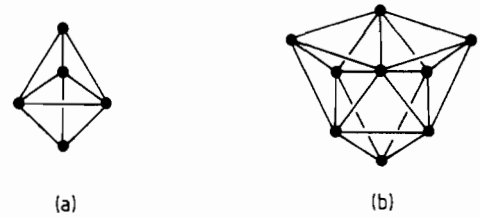

Figure 1. Cluster skeletons of (a) $B_5H_5^{2-}$ and (b) $B_9H_9^{2-}$, which both have D_{3h} symmetry.

As mentioned in the previous section, we cannot formally prove the above theorems for TSH theory cluster orbitals, because the latter lack any higher symmetry beyond that of the point group for which they are constructed. Hence we cannot expect the relative splittings of a cluster orbital manifold, $\psi^\lambda_{L,M}$, to be exactly the same as those of the spherical harmonics, $Y_{L,M}$, in the same potential. However, we would expect the patterns to be qualitatively similar, particularly for L^σ orbitals, which do not involve directional derivatives. The L^π and L^δ cluster orbitals are based upon *tensor* spherical harmonics for which the matrix element theorems discussed above also apply. Hence, we expect their matrix elements and splitting patterns to show similar trends too.

This qualitative similarity is enough for our purposes, since we will not need to use any of the matrix element theorems *quantitatively*. The predictions may also be compared with the results of various molecular orbital calculations. Furthermore there are a number of interesting cases where the frontier orbitals are ψ^σ in character: gold clusters will be treated below, and silicon clusters, in a subsequent paper. Note that the zero-order energy of a cluster orbital manifold is expected to follow the trends observed by Stone[1] for his calculated average cluster orbital energies.

There are two situations of interest that it is helpful to clarify at this point. The first is the case where we do not require all the $2L + 1$ members of a given $\psi^\lambda_{L,M}$ set in the cluster orbital basis. (Recall that the minimal basis set must remain linearly independent under a cluster orbital transformation.) In this case we simply ignore the components that are surplus to requirements after considering the appropriate spherical harmonic splittings. The second (much rarer) case arises when some of the cluster orbitals in a given set are null, e.g. $D^\sigma_{xz,yz,xy}$ for the octahedron. Here again we would expect a qualitative similarity to the splitting of the appropriate spherical harmonic components to remain.

We will now show how this analogy may be used in the correlation of the cluster shape with the molecular orbital energy level spectrum and in the study of rearrangements and electron counts of some gold clusters.

Oblate and Prolate Clusters

We first consider the relation between the shape of a cluster and its energy-level spectrum. Consider the expansion of the electron–nucleus potential energy given above. The point group symmetry of the molecule determines which spherical harmonics appear with nonzero coefficients in this sum; there are more terms in lower order point groups.[10] However, this is not the whole story because we have not yet considered the *magnitude* of the nonzero

(10) Griffith, J. S. *The Theory of Transition Metal Ions*, Cambridge University Press: Cambridge, 1961.
(11) Hoffmann, R.; Gouterman, M. *J. Phys. Chem.* **1962**, *36*, 2189.
(12) Gerloch, M. *Magnetism and Ligand-Field Analysis*, Cambridge University Press: Cambridge, 1983.

terms. This is clearly determined by the degree of distortion of the cluster from spherical symmetry. Consider $B_5H_5^{2-}$ and $B_9H_9^{2-}$ as examples of molecules that both belong to D_{3h} (Figure 1). Considering the positions of the skeletal atoms relative to the principal axis shows that the trigonal bipyramid may be described as prolate (like a rugby ball) while the tricapped trigonal prism is oblate (like a discus). Griffith[10] provides tabulations of the nonzero terms in the potential energy for various point groups including this one, and we will make use of these results below. First, we define real combinations of the spherical harmonics, $Y^c_{L,M}$ and $Y^s_{L,M}$, which are proportional to cos $(M\phi)$ and sin $(M\phi)$, respectively:

$$Y^c_{L,M} = \frac{(-1)^M}{\sqrt{2}}(Y_{L,M} + Y^*_{L,M})$$

$$Y^s_{L,M} = \frac{(-1)^M}{i\sqrt{2}}(Y_{L,M} - Y^*_{L,M}) \qquad (8)$$

where $M > 0$, $i = \sqrt{-1}$, and the asterisk denotes complex conjugation. For D_{3h} the nonzero terms involve $Y_{L,0}$ and $Y^s_{L,3}$ for L even and $Y^c_{L,3}$ for L odd.

Griffith[10] also determines the number of parameters required to describe the splitting of p, d, and f atomic orbitals in a given point group. The same number of parameters will be required for the splitting of a cluster orbital manifold, and can be determined by descent in symmetry tables from the splitting of the P, D, and F irreducible representations of the full-rotation group in the lower symmetry point group. For example, D splits into $A_1 \oplus 2E$ in D_3, so that two parameters are required to describe the relative splittings. One parameter is needed for the t_{2g}–e_g splitting in O_h, and is written as Δ or $10Dq$ for the d orbitals of a transition-metal complex. For a $Y_{2,M}$ manifold ($M = 0, \pm1, \pm2$) in D_{3h} symmetry, there are two terms in the potential responsible for the splitting, and by use of the selection rules for Clebsch–Gordan matrix elements given above, these are easily seen to be $Y_{2,0}$ and $Y_{4,0}$. The relative splittings caused by each term alone are completely determined (in first order) by the Wigner–Eckart theorem. Although these selection rules will not apply quantitatively to the splittings of a set of $D_{2,M}$ cluster orbitals, we expect the same two terms in the potential energy to be the most important.

If all the nuclei are the same distance from the origin, then we may factor out the sum over α, which for the trigonal bipyramid gives

$$\sum_\alpha Y_{2,0}(\theta_\alpha,\phi_\alpha) = \sqrt{\frac{5}{16\pi}}$$

$$\sum_\alpha Y_{4,0}(\theta_\alpha,\phi_\alpha) = 25\sqrt{\frac{9}{256\pi}} \qquad (9)$$

while for $B_9H_9^{2-}$

$$\sum_\alpha Y_{2,0}(\theta_\alpha,\phi_\alpha) = -1.29\sqrt{\frac{5}{16\pi}}$$

$$\sum_\alpha Y_{4,0}(\theta_\alpha,\phi_\alpha) = -11.6\sqrt{\frac{9}{256\pi}} \qquad (10)$$

The ratios of the coefficients for the two terms are therefore 1:−1.29 and 1:−0.46 for $Y_{2,0}$ and $Y_{4,0}$, respectively.

Note that corresponding terms have coefficients of different sign in (9) and (10). This shows how the oblate or prolate nature of a cluster can affect the order of the energy levels because of the different distribution of atoms relative to the nodal surfaces of the spherical harmonics in the potential expansion. This can also be seen if we explicitly consider the addition of the potentials due to the different nuclei. Such an approach has been used in crystal field theory to estimate the d-orbital splittings for a wide range of transition-metal complexes.[13] We shall persue this point in more detail in the following sections.

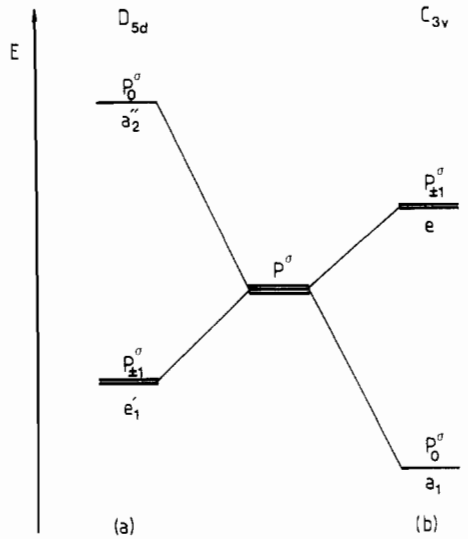

Figure 2. P^σ orbital splittings (schematic) for $Au_7(PPh_3)_7^+$ (left) and $Au_7(PPh_3)_7^{3+}$ (right).[15]

The relative splittings caused by any particular term in the potential expansion are fully determined by the Wigner–Eckart theorem for a set of spherical harmonics because the reduced matrix elements are constant within a given manifold. The Clebsch–Gordan coefficients required are tabulated in various sources,[9] and we will give the results for the five $Y_{2,M}$ functions in the D_{3h} point group. For the $Y_{2,0}$ term the relative splittings are found to be −2:−1:2 for $|M| = 0$, 1, and 2, while for the $Y_{4,0}$ term the ratio is 6:−4:1 in the same order. Note that a barycenter rule applies to these results; e.g., $-2 + 2 \times (-1) + 2 \times 2 = 0$.

To simplify the following discussions, we will concentrate upon the splitting of P^λ cluster orbitals in some axial point groups. For the spherical harmonics we immediately obtain the ratio −2:1 for the relative energies of the a- and e-type orbitals that usually result from this splitting, relative to an energy origin taken at the average energy of the three orbitals, as always. This example is actually very interesting, since the P^σ orbitals lie at the frontier level in a number of spherical and toroidal gold clusters.[14] The relative splittings of the P^σ orbitals have important stereochemical consequences for partially filled shells. In particular, for a two-electron system the geometry which places P^σ_0 below $P^\sigma_{\pm1}$ is favored (by 4β relative to 2β; the P^σ_0 orbital lies at 2β when the $P^\sigma_{\pm1}$ pair lies at $-\beta$, with $\beta < 0$). For four-electron systems the geometry that places the $P^\sigma_{\pm1}$ pair below P^σ_0 is favored (by 4β to 2β). For prolate clusters, P^σ_0 generally lies below $P^\sigma_{\pm1}$ while for oblate clusters the reverse usually holds.

An example where an inversion of the P^σ orbitals can be seen occurs in going from pentagonal bipyramid (oblate) to a capped octahedron (prolate). The orbital splittings of P^σ for these two examples are shown in Figure 2, and extended Hückel calculations[15] indicate that for $Au_7(PPh_3)_7^+$ the oblate geometry is preferred, while the prolate geometry is preferred for $Au_7(PPh_3)_7^{3+}$, in agreement with the sense of the P^σ splitting deduced below.

These ideas are also relevant to understanding the geometries of alkali-metal clusters. Li_8 is calculated to have a "spherical" tetracapped tetrahedral geometry corresponding to the occupation of S^σ and the three P^σ cluster orbitals.[16] In contrast Li_6 is predicted to have a planar D_{3h} raft geometry (oblate).

We will now consider in more detail the distortion of a trigonal antiprism into a chair while D_{3d} symmetry is maintained (Figure 3). The two clusters are related by stretching along the 3-fold

(13) Krishnamurphy, R.; Schaap, W. B. *J. Chem. Educ.* **1969**, *46*, 799.
(14) Hall, K. P.; Gilmour, D. I.; Mingos, D. M. P. *J. Organomet. Chem.* **1984**, *268*, 275. Briant, C. E.; Wheeler, A. C.; Mingos, D. M. P. *J. Chem. Soc., Chem. Commun.* **1984**, 248.
(15) Evans, D. G.; Mingos, D. M. P. *J. Organomet. Chem.* **1985**, *295*, 389.
(16) Koutecký, J.; Fantucci, P. *Z. Phys. D* **1986**, *3*, 147.

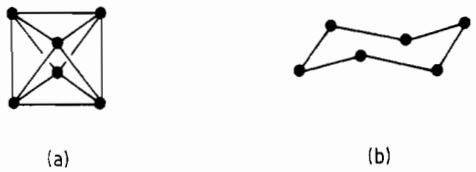

Figure 3. D_{3d} cluster skeletons: (a) the trigonal antiprism; (b) the "chair". The two are related by a distortion along the 3-fold axis.

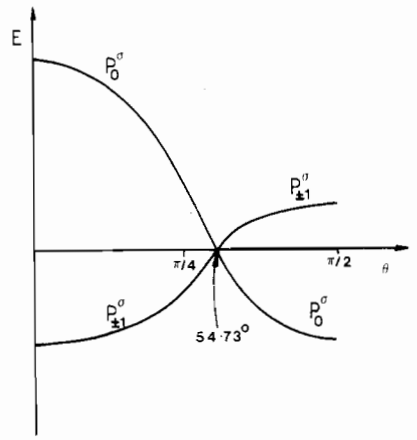

Figure 4. Variation of the P^σ energies with θ for the trigonal-antiprism → chair distortion (by analogy with the splitting of $Y_{1,M}$ ($M = \pm1, 0$)).

principal axis, and the same nonzero terms arise in the expansion of the potential energy as for the D_{3h} *closo*-boranes above. For P^λ cluster orbitals, the analogy with the matrix elements of $Y_{1,M}$ ($M = 0, \pm1$) suggests that the terms involving $Y_{2,0}$ will be the most important (all the others vanish for $Y_{1,M}$ because of the triangle selection rule on the Clebsch–Gordan coefficients). Hence we consider

$$-\sum_\alpha \frac{Z_\alpha}{r_{i\alpha}} = -4\pi\sum_\alpha Z_\alpha\left(\frac{1}{r_{i>}} + \frac{r_{i<}^2}{5r_{i>}^3}Y_{2,0}(\theta_\alpha,\phi_\alpha)\ Y_{2,0}(\theta_i,\phi_i) + \ldots\right) \quad (11)$$

The structural factor that is expected to determine the magnitude of the cluster orbital splittings is therefore $\sum_\alpha(3\cos^2\theta_\alpha - 1)$, or simply $(3\cos^2\theta - 1)$ since all the vertex atoms have the same $\cos^2\theta_\alpha$. This factor is positive in the region $0° < \theta < 54.73°$ and negative for $54.73° < \theta < 90°$. Hence as θ passes through $\cos^{-1}(1/\sqrt{3}) = 54.73°$ the splitting of the P^σ set should reverse. At the critical angle, all three energy levels are degenerate because the cluster then has octahedral symmetry. The determination of the sense of the splitting is quite straightforward, as discussed in the next section. P_z^σ is the high-lying inaccessible orbital for the "chair" structure, while the $P_{x,y}^\sigma$ set is higher lying in the trigonal antiprism (Figure 4) as can be seen by considering the effect on P_z^σ of pulling the two triangles of atoms apart to a large distance.

The skeletal bonding orbitals for the toroidal gold cluster $Au_7(PPh_3)_6^+$ (Figure 5a) are calculated to be S^σ and $P_{x,y}^\sigma$,[14] in agreement with the above analysis. In fact, Mingos has shown that all centered toroidal gold clusters have occupied S^σ and $P_{\pm1}^\sigma$ cluster orbitals and $12n_s + 16$ valence electrons, where n_s is the number of gold atoms in the ring.[17] The 16 electrons arise from a filled d shell on the central gold atom and occupation of S^σ and $P_{\pm1}^\sigma$. Examples of gold clusters that conform to this generalization include $Au_9(P(p\text{-}C_6H_4OMe)_3)_8^{3+}$ (crown, Figure 5b) and $Au_9(PPh_3)_8^{3+}$ (icosahedron minus two pairs of adjacent atoms, Figure 5c). In pseudospherical gold clusters the three P^σ cluster orbitals are approximately degenerate and there are $12n_s + 18$ valence electrons. Examples of such clusters include $Au_8(PPh_3)_8^+$ (distorted cube, Figure 5d) and $Au_{13}Cl_2(PMe_2Ph)_{10}^{3+}$ (icosahedron).

Note that the inversion of order is due to the cluster vertices crossing the nodal cone of $Y_{2,0}$ at $\theta = 54.37°$. It is precisely this

(17) Hall, K. P.; Mingos, D. M. P. *Prog. Inorg. Chem.* **1984**, *32*, 237.

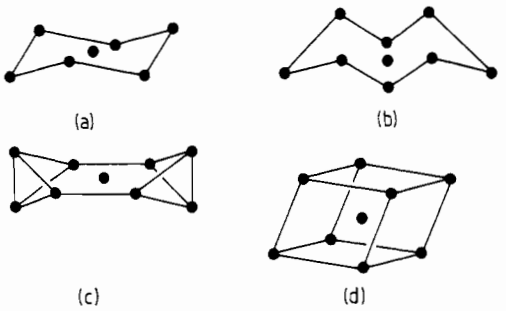

Figure 5. Gold skeletons of (a) $Au_7(PPh_3)_6^+$, (b) $Au_9(P(p\text{-}C_6H_4OMe)_3)_8^{3+}$, (c) $Au_9(PPh_3)_8^+$, and (d) $Au_8(PPh_3)_8^{3+}$.

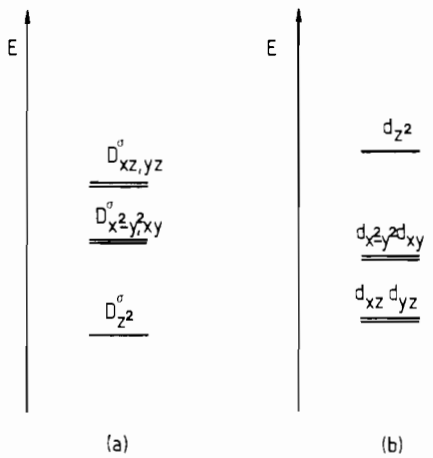

Figure 6. The splitting of a set of D^σ orbitals in a trigonal-bipyramidal cluster (a) is expected to be inverted with respect to the splitting of a set of d atomic orbitals on the central metal atom in a complex with the same symmetry (b).

sort of feature that will often lead to different relative orderings of levels in prolate and oblate molecules. As we have seen above, this ordering may be of great importance for orbitals at the frontier level.

Determination of the Order of the Energy Levels

In the previous section we noted that the inversion of the a and e symmetry orbitals derived from P^σ is of great significance for electron counting in gold clusters. Hence, it is a matter of some importance to determine which way around this splitting will be.

For L^σ cluster orbitals this question may be answered by comparison with the atomic orbital splittings in a transition-metal complex. In the simplest crystal field model, we would simply consider the spatial characteristics of the atomic orbitals in question relative to the positions of the ligands, modeled as point negative charges. Orbitals with a large amplitude in the proximity of one or more ligands would be expected to suffer a relatively large Coulombic repulsion and consequently to be high lying. For L^σ orbitals the same considerations may be applied except that the electron–nucleus potential is *attractive* rather than repulsive. For example, the angular characteristics of a set of D^σ orbitals are the same as those of a set of d orbitals on a central transition-metal atom in a complex. Hence we expect an inversion of the splittings of L^σ with respect to the l atomic orbitals in a complex with σ-donor ligands in the same arrangement as the cluster vertices (Figure 6).

For L^π and L^δ cluster orbitals, the situation is complicated by the directional character of the functions involved, and the splitting may not be in the same sense as the L^σ orbitals. Instead we would expect the patterns to be related to those of the appropriate *tensor* spherical harmonics. For example, the L^π orbitals have their maximum amplitude at the nodes of L^σ (because this is where the gradient of $Y_{L,M}$ is largest), but it is still the nodal distribution of the parent spherical harmonic relative to the vertex sites that is most important. If we consider P_z^σ and P_z^π for a trigonal prism, it is clear that the cross-equator interaction is antibonding in both

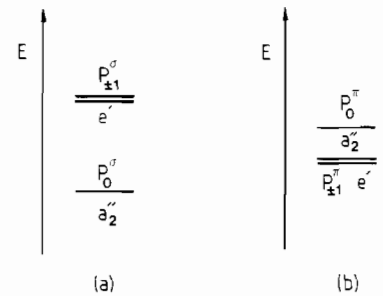

Figure 7. P^{λ} splittings in the trigonal prism: (a) P^{σ}; (b) P^{π}.

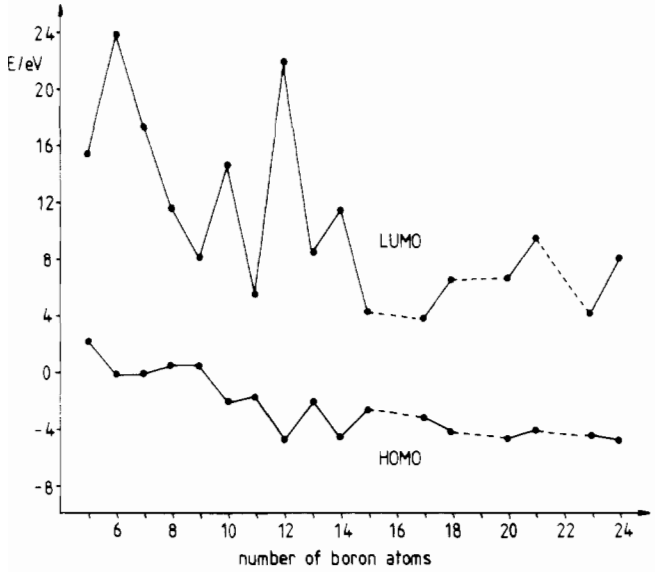

Figure 8. Plot of calculated HOMO and LUMO energies in the $B_nH_n^{2-}$ series.

cases. However, when the in-plane interaction is included[6] we find that P^{σ}_{z} lies lower than $P^{\sigma}_{x,y}$ while P^{π}_{z} lies higher than $P^{\pi}_{x,y}$ (Figure 7).

Application to Cluster Rearrangements

Above, we considered the energy level spectra of toroidal (oblate) and spherical (prolate or oblate) gold clusters and found that the P^{σ} frontier orbitals are typically split in different senses in the two sets. It follows that skeletal rearrangements that involve a change in *shape* in the transition state may be unfavorable due to orbital crossings or avoided crossings, as discussed in detail elsewhere.[18]

Since all these gold clusters are known to be fluxional, it follows that the mechanisms will involve no qualitative change of shape.[18] For example, the pentagonal-bipyramidal gold cluster $Au_7(PPh_3)_7^+$ (oblate) is not expected to rearrange in a double diamond–square–diamond process via the capped octahedron (prolate). Instead a "local bond rotation"[19] may be responsible for the observed fluxionality, since the cluster remains approximately oblate throughout this process.

Application to *closo*-Boranes

For the smaller *closo*-borohydrides, $B_nH_n^{2-}$, it is well-known both theoretically and experimentally that species with an odd number of boron atoms are generally less stable than their even-numbered counterparts.[20] A plot of the calculated HOMO and LUMO energies for $B_5H_5^{2-}$ up to $B_{24}H_{24}^{2-}$ (excluding those molecules with deviations from the $n + 1$ skeletal electron count) is given in Figure 8. This shows that in terms of the HOMO–LUMO gap this stability trend may extend to the hypothetical species too; there is also a steady decrease in the HOMO–LUMO gap with increasing n, as expected. If we compare $B_nH_n^{2-}$ with $B_{n+1}H_{n+1}^{2-}$ for each relevant pair of neighbors, we find that the HOMO–LUMO gap usually rises if n is even and falls if n is odd, despite the underlying trend downward.

Table I. Correlation between Point Group and HOMO–LUMO Gap in the $B_nH_n^{2-}$ Series

n	5	6	7	8	9	10	11	12
Point group	D_{3h}	O_h	D_{5h}	D_{2d}	D_{3h}	D_{4d}	C_{2v}	I_h
HOMO-LUMO gap/eV	14	26	18.7	12	8	18	8	28.7

n	13	14	15	17	18	20	21	23	24
Point group	C_{2v}	D_{6d}	D_{3h}	C_{2v}	D_3	D_{6h}	D_3	D_3	T
HOMO-LUMO gap/eV	11.5	17.3	7.7	7.5	11.7	12	14.5	9.3	14

These gaps were calculated by using the Fenske–Hall method,[21] and the hypothetical molecules (with more than 12 vertices) have been the subject of several previous studies.[22,23] The geometries used were identical with those of Fowler,[23] and the results verify the conclusions of the previous studies: the hypothetical molecules are expected to be electronically stable. (Deviations from the usual $n + 1$ skeletal electron pairs occur due to the detailed symmetry of some species.) The reason for the nonexistence of these higher *closo*-boranes is therefore not electronic; in fact, the answer probably lies in the dynamics of cluster growth, as discussed elsewhere.[24]

The trends observed in Table I may be explained by considering three factors. First, note that there is a strong correlation between the point group symmetry of any given molecule in this series and its HOMO–LUMO gap. Clearly, the higher the order of the point group, the more closely the cluster is likely to approximate to a sphere. For molecules belonging to high-symmetry point groups, the basis atomic orbitals will in general span a larger number of different irreducible representations (IRs) than those for less symmetrical species. In low-symmetry molecules, the mixing of the frontier orbitals with other orbitals of the same symmetry can raise the HOMO in energy and lower the LUMO, resulting in a smaller gap. Second, for larger clusters there is more mixing between orbitals transforming according to the same IR, simply because of the increase in dimension of the basis.

The third factor is the shape of the cluster. The *closo*-boranes considered in this section, except for the octahedron and icosahedron, usually oscillate between prolate and oblate geometries. As explained above, the point group symmetry of the molecule determines which spherical harmonics appear with nonzero coefficients in the expansion of the electron–nucleus potential energy. For lower symmetry clusters, there are more nonzero terms whose magnitude is a measure of the distortion from spherical symmetry. Furthermore, by analogy with the spherical harmonics, we expect only a few of the nonzero terms to produce most of the splitting. In fact we should probably compare the splitting of an L^{π} manifold with that of the vector spherical harmonic $\mathbf{Y}_{L,M} = (\nabla Y_{L,M}\cdot\mathbf{e}^{\theta})\mathbf{e}^{\theta} + (\nabla Y_{L,M}\cdot\mathbf{e}^{\phi})\mathbf{e}^{\phi}$ as defined by the integral $\int \mathbf{Y}_{L,M}\cdot\mathbf{Y}^{*}_{L,M} V\,d\tau$, which is a scalar integral over all space. Unfortunately the latter splittings are not as easily visualized as those of the spherical harmonics themselves. Nonetheless there are certainly some trends for the HOMO–LUMO gaps of the *closo*-boranes in Table I that are suggestive of a simple splitting pattern. The most obvious feature is the large gaps observed for "spherical" clusters where all the vertices are equivalent, i.e. the octahedron and the icosahedron. This is probably due to factors one and two, above. However, clusters with the $L^{\pi}_{\pm1}$ members of the outer L^{π} manifold (that is the one with the largest L) occupied also have large gaps. Examples are the trigonal bipyramid (five

(18) Wales, D. J.; Mingos, D. M. P.; Zhenyang, L. *Inorg. Chem.*, following paper in this issue. Wales, D. J.; Mingos, D. M. P. *Polyhedron*, in press.
(19) McKee, M. L. *J. Am. Chem. Soc.* **1988**, *110*, 5317.
(20) Todd, L. J. *Prog. Boron Chem.* **1970**, *2*, 10.
(21) Fenske, R. F.; Caulton, K. G.; Radtke, D. D.; Sweeney, C. C. *Inorg. Chem.* **1966**, *5*, 951. Fenske, R. F.; Radtke, D. D. *Inorg. Chem.* **1968**, *7*, 179. Fenske, R. F.; DeKock, R. L. *Inorg. Chem.* **1970**, *9*, 1053. Hall, M. B.; Fenske, R. F. *Inorg. Chem.* **1972**, *11*, 768.
(22) Brown, L. D.; Lipscomb, W. N. *Inorg. Chem.* **1977**, *16*, 2989. Bicerano, J.; Marynick, D. S.; Lipscomb, W. N. *Inorg. Chem.* **1978**, *17*, 2041, 3443.
(23) Fowler, P. W. *Polyhedron* **1985**, *4*, 2051.
(24) Wales, D. J. *Chem. Phys. Lett.* **1987**, *141*, 478.

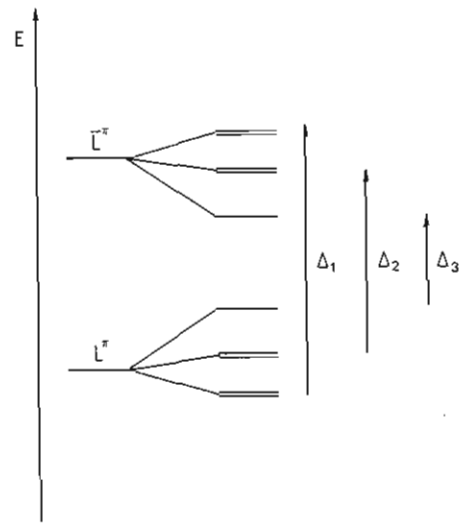

Figure 9. Splitting patterns for the outer L^{π} manifold suggested by the HOMO–LUMO gaps of $B_5H_5^{2-}$, $B_7H_7^{2-}$, $B_{10}H_{10}^{2-}$, and $B_{14}H_{14}^{2-}$. The gaps expected for three possible occupations of these orbitals are marked.

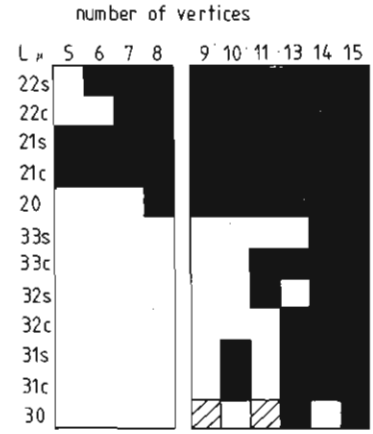

Figure 10. Occupation of the D^{π} and F^{π} orbitals for *closo*-boranes with 5–15 vertices. The icosahedron is omitted because symmetry-adapted linear combinations of these functions are needed in this case. The alternative (hatched lines) shading indicates that it is the odd cluster orbital which is actually occupied. Note that the choice of cluster orbitals within a given incomplete L^{π} manifold is not always unique.

vertices) and the bicapped square antiprism (ten vertices). This could be explained if the splitting of the L^{π} orbitals in these sets leaves these two orbitals low-lying, as illustrated in Figure 9. Furthermore, clusters with a single member of the outer L^{π} manifold unoccupied also have relatively large HOMO–LUMO gaps. Examples are the pentagonal bipyramid (seven vertices, $D^{\pi}_{\pm 1}$ and $D^{\pi}_{\pm 2}$ occupied) and the 14-atom D_{6d} symmetry structure ($F^{\pi}_{\pm 1}$, $F^{\pi}_{\pm 2}$, and $F^{\pi}_{\pm 3}$ occupied). This could again be explained if the splitting resulted in a relatively high-lying L^{π}_0 orbital, as in Figure 9. This might be caused by the nodal surfaces of $Y_{L,0}$, which can be written as θ = constant, bisecting more edges in these clusters than those of the other members of the $Y_{L,M}$ set (which always include nodal planes of the form ϕ = constant).

We also note that a relatively small HOMO–LUMO gap occurs for $B_8H_8^{2-}$ in which the outer D^{π} shell is filled. The F^{π} shell is precisely filled at the 15-vertex D_{3h} structure, which also has a relatively small gap. The nine-vertex tricapped trigonal prism is particularly interesting since the HOMO belongs to the $\bar{F}^{\pi}$ set. A small gap results in this case because the F^{π} and $\bar{F}^{\pi}$ sets overlap, probably because this cluster is actually not very spherical. Overlap also occurs for the 11-vertex deltahedron, which also has a relatively small gap, again indicating a splitting pattern with L^{π}_0 high lying. Of course, we should not try to stretch this pattern too far, since factors one and two (above) must also be important. The occupation of the D^{π} and F^{π} orbitals is summarized for the *closo*-boranes with 5–15 vertices in Figure 10.

How does this analysis compare with the experimental data[20] for the *closo*-boranes? A small HOMO–LUMO gap may result in greater reactivity and an inherent *kinetic* instability; nucleophiles will attack the low-lying LUMO, and electrophiles will attack the high-lying HOMO. This may also be interpreted in terms of the point group symmetry and charge distribution of the molecule; in a low-symmetry species the electronic environments of some vertex atoms are inherently different, leading to polarity and increased reactivity. The charge distribution in a cluster may also be discussed conveniently within the TSH theory framework. The main factors of importance are the coordination numbers and the molecular orbital occupation. In $B_8H_8^{2-}$, for example, the occupied L^{π} set consists entirely of the filled subshells P^{π} and D^{π}, but this is not usually the case in most other clusters, and the observed charge distributions can be attributed to differences in connectivity. The presence of partially filled L^{π} subshells must obviously reflect the point group symmetry of the molecule and the charge distribution.[25] For the D^{π} manifold an unoccupied orbital leads to a depletion of electron density in a fairly obvious manner. It is helpful to note that filled $D^{\pi}_{xz,yz,xy}$ and $D^{\pi}_{x^2-y^2,z^2}$ sets have full cubic symmetry in the octahedral point group. For example, in the prolate trigonal-bipyramid $B_5H_5^{2-}$, where $D^{\pi}_{xz,yz}$ orbitals are occupied, there is a depletion of electron density in the xy plane and an increase on the z axis due to the absence of D^{π}_{xy}. In contrast, for the oblate pentagonal-bipyramid $B_7H_7^{2-}$ only the $D^{\pi}_{z^2}$ orbital is not required, and there is a buildup of electron density in the xy plane. These results are illustrative of the more general principle that negative charge often builds up at points of lowest connectivity in a cluster, and the cluster orbital basis set must reflect this distribution. When this observation is combined with first-order perturbation theory, it is possible to predict the more stable isomers for, e.g., carboranes.[26] For example, in $C_2B_3H_5$ (prolate) the most stable isomer has the carbon atoms at the poles, whereas for $C_2B_5H_7$ (oblate) the carbon atoms are equatorial in the most stable isomer.

These borane calculations also enable us to examine some previously derived estimates for the bonding trends followed by even and odd π cluster orbitals with increasing cluster nuclearity.[6] The critical value of the TSH "quantum number" L for which odd π orbitals are expected to become bonding in a regular polyhedron of coordination number λ is given by

$$L_c \approx \lambda/2$$

where λ is the coordination number of the vertices within the cluster skeleton. This enables us to estimate the cluster nuclearity, n, at which the odd and even π orbitals may begin to overlap,[3] we find that $\sqrt{(n+1)} \approx \lambda/2 + 1$. This is likely to be an underestimate for less regular clusters because the number of edges increases more rapidly than the average coordination number.

The percentage of odd π orbital character in the occupied frontier levels was indeed found to increase along the series $B_{13}H_{13}^{2-}$ to $B_{24}H_{24}^{2-}$. However, the changes involved are smaller than would be expected from the crude estimate of odd–even π-orbital overlap above. This should not surprise us, since the number of nearest-neighbor contacts in these molecules rises as $3n - 6$, where n is the number of vertices, which is significantly faster than the increase in average coordination number when compared to regular polyhedra. (The number of nearest-neighbor contacts may be readily derived by noting that these species have 12 five-coordinate and $n - 12$ six-coordinate vertices.)

However, node-counting arguments of the above type can provide some useful insight at a more qualitative level. A

(25) Mingos, D. M. P.; Hawes, C. *Struct. Bonding* **1985**, *63*, 1. Mingos, D. M. P. *Pure Appl. Chem.* **1987**, *59*, 145.

(26) Gimarc, B. M.; Ott, J. J. *J. Am. Chem. Soc.* **1986**, *108*, 4298.

Fenske-Hall calculation on $B_{32}H_{32}^{2-}$ shows that the HOMO has T_{1g} symmetry and belongs to the odd $\bar{H}^{\pi}$ set of π orbitals. Its conjugate T_{1u} partner, belonging to the H^{π} set, is the LUMO of this cluster, and lies about 1 eV above the HOMO. Hence we see that for this highly symmetrical species, with only two types of vertex atom, the odd and even π sets do indeed overlap.

Conclusions

In this paper we have discussed the splitting of cluster orbitals using the framework of Stone's tensor surface harmonic (TSH) theory. Although the TSH theory cluster orbitals do not transform like their parent spherical harmonics under *arbitrary* rotations, we still expect the splitting patterns to be qualitatively similar. In particular, when the electron-nucleus potential energy is expanded in spherical harmonics a center-of-gravity rule may be deduced for the first-order splitting of the spherical harmonics, $Y_{L,M}$, by the non spherically symmetric part of the Hamiltonian.

The splittings of cluster orbitals are found to depend upon the relation between the nodal surfaces of the nonzero terms in the spherical harmonic expansion and the cluster vertices. Hence we have discussed the relation between the *shape* of a cluster and its energy level spectrum with particular reference to the *closo*-borohydrides. The shape of the molecule determines the *sense* of the cluster orbital splittings as well as the *magnitude* of the nonzero terms in the potential energy expansion. These expectations are illustrated by the different electron counts of toroidal and spherical gold clusters and are also expected to influence the skeletal rearrangements of these species.

Some of the techniques used have direct analogies in crystal field theory. In particular, a set of L^{σ} cluster orbitals should be split in the opposite sense to a set of l atomic orbitals on the central atom of a complex with ligands in the same arrangement as the cluster vertices.

In fact, there is another center-of-gravity rule that applies to complete sets of, e.g., σ and π cluster orbitals. If each orbital in an interacting set has the same self-energy, α, then one can easily prove that there is a center-of-gravity relative to $\alpha = 0$.

Acknowledgment. D.J.W. thanks Downing College Cambridge for financial support for his visit to Oxford, during which this work was performed, and Dr. D. W. Fowler for his borane coordinates.

Registry No. Borane, 13283-31-3.

Contribution from the Department of Chemistry, University of Chicago, 5735 South Ellis Avenue, Chicago, Illinois 60637, and Inorganic Chemistry Laboratory, University of Oxford, South Parks Road, Oxford OX1 3QR, United Kingdom

Skeletal Rearrangements in Clusters. 2.

David J. Wales,*[†] D. Michael P. Mingos,[‡] and Lin Zhenyang[‡]

Received January 23, 1989

In this paper, we continue a theoretical study of the rearrangements of cluster skeletal atoms with emphasis on the possible differences between transition-metal and main-group clusters. We show that the selection rules for orbital-symmetry-forbidden "TSH-forced" crossings, derived for main-group clusters using Stone's tensor surface harmonic (TSH) theory, should also be applicable to transition-metal clusters as long as the metal fragments are isolobal to B-H. We also discuss the feasibility of various single edge-cleavage mechanisms that were not previously considered for main-group clusters in part 1. Using TSH theory and polyhedral skeletal electron pair theory[1] electron-counting rules, especially for "capping" and "condensation" principles, we find that most of the new processes recently suggested in another study are probably unfavorable. Some alternative mechanisms are therefore suggested, with particular attention being paid to the new possibilities predicted for transition-metal clusters.

Introduction

The theoretical study of rearrangements in cluster compounds has recently been elegantly analyzed with use of Stone's tensor surface harmonic (TSH) theory.[2-6] The new approach, due to Wales and Stone[7] (part 1 in this series), enables some rearrangement processes that have an orbital crossing, and are therefore "forbidden" in the Woodward-Hoffmann sense,[8] to be identified very simply. The analysis in part 1 explained, in terms of TSH theory, why Lipscomb's diamond-square-diamond (DSD) process[9] (illustrated in Figure 1) should in principle be energetically favorable and identified some special cases where it is not. It was built partly upon King's topological considerations, which distinguish between inherently rigid clusters (containing no *degenerate* edges) and those for which one or more DSD processes are *topologically* feasible.[10] An edge is termed *degenerate* if a DSD process in which it is broken leads to a product with the same cluster skeletal geometry as the starting molecule.

The conclusion of part 1 was that transition states between *closo*-boranes or *closo*-carboranes with a single atom on a principal rotation axis of order three or more will generally have an orbital crossing and hence be high-energy processes.[11] The effect of lower symmetry environments, for example, when there is a single atom on a 2-fold axis, was also considered. In this case, the barrier to rearrangement may also be large, depending upon the splitting of the HOMO and LUMO, which form a degenerate pair of E symmetry when the principal axis is of higher order. Substituents around the critical face at which the DSD process occurs may help to lower the barrier by increasing the difference between the electronic environments in the local x and y directions, and hence increasing the HOMO-LUMO gap.[7]

Independently, Johnston and Mingos recognized that for *closo*-boranes, $B_nH_n^{2-}$, with $4p + 1$ atoms, i.e. $B_5H_5^{2-}$ and $B_9H_9^{2-}$, the single DSD process is symmetry forbidden because a mirror plane is retained throughout.[12] In contrast, single DSD processes in which only a C_2 symmetry element is conserved, e.g. for $B_8H_8^{2-}$, do not involve a crossing and are symmetry allowed. This symmetry rule has its origins in the nodal characteristics of L^{π} and $\bar{L}^{\pi}$ cluster orbitals and their behavior under the symmetry op-

[†] University of Chicago.
[‡] University of Oxford.

(1) Mingos, D. M. P. *Acc. Chem. Res.* **1984**, *17*, 311.
(2) Stone, A. J. *Mol. Phys.* **1980**, *41*, 1339.
(3) Stone, A. J. *Inorg. Chem.* **1981**, *20*, 563.
(4) Stone, A. J.; Alderton, M. J. *Inorg. Chem.* **1982**, *21*, 2297.
(5) Stone, A. J. *Polyhedron* **1985**, *3*, 1299.
(6) Stone, A. J.; Wales, D. J. *Mol. Phys.* **1987**, *61*, 747.
(7) Wales, D. J.; Stone, A. J. *Inorg. Chem.* **1987**, *26*, 3845.
(8) Woodward, R. B.; Hoffmann, R. *Angew. Chem., Int. Ed. Engl.* **1969**, *8*, 781.
(9) Lipscomb, W. N. *Science (Washington, D.C.)* **1966**, *153*, 373.
(10) King, R. B. *Inorg. Chim. Acta* **1981**, *49*, 237.
(11) Gimarc, B. M.; Ott, J. J. *Inorg. Chem.* **1986**, *25*, 83, 2708.
(12) Johnston, R. L.; Mingos, D. M. P. *Polyhedron*, in press.

0020-1669/89/1328-2754$01.50/0 © 1989 American Chemical Society